Inorganic Chemistry

ARTICLE

pubs.acs.org/IC

Pressure-Induced Formation of Molecular $B_2X_4(\mu\text{-}X)_2$ (X = Cl, Br, I) Species

Serguei Patchkovskii, Dennis D. Klug, and Yansun Yao*

Steacie Institute for Molecular Sciences, National Research Council of Canada, 100 Sussex Drive, Ottawa, Canada K1A 0R6

ABSTRACT: Boron(III) halides (BX_3, where X = F, Cl, Br, I) at ambient pressure conditions exist as strictly monomeric, trigonal-planar molecules. Using correlated ab initio calculations, the three heavier halides (X = Cl, Br, I) are shown to possess $B_2X_4(\mu\text{-}X)_2$ local minima, isostructural with the diborane molecule. The calculated dissociation barrier of the $B_2I_4(\mu\text{-}I)_2$ species [≈14 kJ/mol with CCSD(T)/cc-pVTZ] may be high enough to allow cryogenic isolation. The remaining dimer structures are more labile, with dissociation barriers of less than 6 kJ/mol. All three dimer species may be stabilized by application of external pressure. Periodic density functional theory calculations predict a new dimer-based $P\bar{1}$ solid, which becomes more stable than the $P6_3/m$ monomer-derived solids at 5 (X = I) to 15 (X = Cl) GPa. Metadynamics simulations suggest that $B_2X_4(\mu\text{-}X)_2$-based solids are the kinetically preferred product of pressurization of the $P6_3/m$ solid.

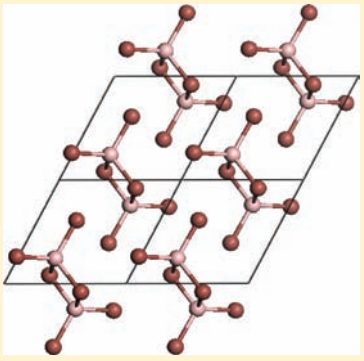

INTRODUCTION

Unlike their subhalide cousins,[1] boron(III) halide chemistry is somewhat unexciting, with the last new binary species reported over 15 years ago.[2−4] In contrast to the stable monomeric BX_3 (X = F, Cl, Br, I), the multinuclear boron(III) halides are too unstable to be isolated in bulk and have been identified from perturbations in spectra of the dominant monomer species. Boron fluoride forms a weakly bound C_{2h}-symmetric van der Waals dimer, with a calculated gas-phase heat of formation of −4[5] or −9[6] kJ/mol. It has been identified in IR spectra of cold matrixes.[4] Both $(BCl_3)_2$ and $(BBr_3)_2$ species have been deduced from Raman spectra of the corresponding monomeric liquids[2,3] and are believed to be Lewis-type donor−acceptor structures with a single bridging halogen atom. The experimental heats of formation are again very small: −0.52 ± 0.08 kJ/mol for $(BCl_3)_2$[3] and −0.9 ± 0.8 kJ/mol for $(BBr_3)_2$.[2] To the best of our knowledge, no other polynuclear forms of BF_3, BCl_3, or BBr_3 have ever been reported. Although BI_3 polymerizes upon standing,[7] the polymers have never been characterized, and no oligomers of BI_3 are present in the gas phase.[8] The textbook summary of binary boron(III) halides chemistry is thus[7] "... the boron trihalides are strictly monomeric, trigonal planar molecules."

Under ambient pressure, boron trihalides form isomorphous hexagonal structures described by the $P6_3/m$ space group with two molecules in the unit cell.[9,10] Recently, several studies of Raman spectroscopy, X-ray diffraction, and electric conductivity of BBr_3 and BI_3 solids under pressure have appeared in the literature.[11,12] So far, structures of these high-pressure solids have not been fully characterized, although a new structure of BI_3 has been reported to form at pressures above 6.2 GPa.[12] A recent density functional theory (DFT) study[13] has predicted a $B_2I_4(\mu\text{-}I)_2$ molecular solid structure to form at high pressure. This structure is consistent with all of the basic features of the experimental study,[12] suggesting that the first new pure-phase binary trihalide of boron has been prepared in more than a century. (The last of the binary boron(III) halides, BI_3, has been known since 1891.[14])

So far, it remains unclear whether the $B_2I_4(\mu\text{-}I)_2$ species is sufficiently stable to be recovered at ambient conditions. It is also not known whether lighter halides can dimerize in the same way under pressure. The objective of this study is to explore gas-phase dimer formation and decomposition with correlated ab initio calculations. Using structural search techniques in combination with periodic DFT, it is demonstrated that $B_2X_4(\mu\text{-}X)_2$ (X = Cl, Br, I) species can be formed by pressurization of the corresponding $P6_3/m$ BX_3 solids.

METHODS

Gas-phase heats of formation and activation energies were calculated using the cc-pVTZ basis set[16] on B, F, and Cl atoms and the cc-pVTZ-PP basis set[17] on Br and I atoms. Small-core scalar-relativistic energy-consistent pseudopotentials[17] were used on Br and I atoms. All energy minima were optimized at the correlated single-reference MP2 level and confirmed as minima or saddle points using harmonic vibrational analysis. The calculated heats of formation and reaction barriers include the zero-point vibrational correction (zero-point energy, ZPE), calculated from the unscaled MP2 harmonic vibrational frequencies. For saddle points, imaginary-frequency normal modes were excluded from the ZPE evaluation. Correlation effects beyond the MP2 level were estimated via single-point CCSD(T) calculations using the cc-pVDZ/cc-pVDZ-PP basis set. The difference between the CCSD(T) and MP2 total energies was assumed to be additive. The resulting correlation correction is negligible for the fluorine species but becomes progressively important for heavier halogens. As an accuracy check for this correction procedure, the $B_2I_4(\mu\text{-}I)_2$ geometry, heat of formation,

Received: July 30, 2011
Published: September 21, 2011

and dissociation barrier were recalculated at the CCSD(T)/cc-pVTZ-PP level. The corresponding ZPE corrections were determined at the CCSD/cc-pVDZ-PP level. Coupled-cluster geometry optimizations and Hessian calculations employed the *CFOUR*[18] coupled-cluster package. All remaining calculations were performed using *GAMESS-US*.[19]

Solid-state structural optimizations and total energy calculations were performed on the low-pressure $P6_3/m$ and predicted high-pressure $P\bar{1}$ structures using the Vienna ab initio simulation (VASP) program[20] and the projected augmented wave potential with the Perdew−Burke−Ernzerhof (PBE) exchange-correlation functional.[21] The gas-phase structures and relative energies of the mono- and binuclear boron(III) halides predicted by this functional are in good agreement with correlated ab initio results, lending additional confidence in the results of solid-state simulations. The predicted high-pressure $P\bar{1}$ crystal structures for the BX_3 boron trihalides were obtained from a detailed structural search of candidate structures for BI_3 based on the initial structural data of Hamaya et al.[12,13] The B, I, Br, and Cl potentials used $2s^22p^1$, $5s^25p^5$, $4s^24p^5$, and $3s^23p^5$ as valence states, respectively, and an energy cutoff of 500 eV.

Phonon calculations were performed using the *ABINIT* program[22] employing the linear response method, Trouiller-Martins-type[23] pseudopotentials with an energy cutoff of 40 hartree, a generalized gradient approximation, and the PBE exchange-correlation functional. An $8 \times 8 \times 8$ *k*-point mesh was used for Brillouin zone (BZ) sampling for phonon calculations. Phonon calculations for the low-symmetry $P\bar{1}$ structure were performed at the boundary points of the BZ for this space group.

RESULTS AND DISCUSSION

According to the MP2 calculations, all four B_2X_6 gas-phase species possess stable doubly bridged local minima with the $B_2X_4(\mu\text{-}X)_2$ bonding motif. The calculated B−X distances are consistent with covalent bonds between both B atoms and the bridging halogens (see Table 1). The B_2F_6, B_2Cl_6, and B_2Br_6-optimized MP2 structures are similar to the previously reported[5,6,15] Hartree−Fock (HF) structures. However, the D_{2h} MP2 structure of B_2F_6 is found to be a shallow local minimum rather than a saddle point, as seen for restricted HF.[5,6] For the heavier halogens (Cl, Br, I), the van der Waals interaction between terminal halogen atoms becomes increasingly more important, causing the formation of two equivalent C_{2v} minima, connected by the D_{2h} saddle point. For the B_2Cl_6 species, the CCSD(T) residual correlation energy correction reverses the relative stability of the D_{2h} and C_{2v} structures. However, the energy difference between the structures in B_2Cl_6 is extremely small (less than 0.2 kJ/mol) and cannot be reliably determined at the level of theory used presently.

Although covalent dimerization of all four BX_3 species is predicted to be energetically unfavorable in the gas phase, the dimers may still be metastable if their dissociation requires overcoming a significant activation barrier. The relative energies and key structural parameters of the lowest-energy transition structures (TSs) for dimer dissociation are given in Table 2. It has proven impossible to locate a meaningful TS for dissociation of $B_2F_4(\mu\text{-}F)_2$. The covalent minimum of the potential energy surface (PES) of this species is connected to the well-known van der Waals dimer[4−6] by an essentially barrierless reaction path, with the maximum energy along the path within 0.1 kJ/mol of the D_{2h} minimum.

Small, but non-negligible barriers were found for the three heavier halogens. For Cl and Br, the TS possesses C_2 symmetry, with two opposing B−X bonds being broken simultaneously. Their corresponding activation energies are 2.5 and 6.3 kJ/mol, respectively.

A more substantial barrier of 14.1 kJ/mol (CCSD(T); 23.8 kJ/mol MP2) is found for the C_2 B_2I_6 saddle point. However, the C_2 structure corresponds to a second-order saddle point on the MP2 PES. Further geometry relaxation yields two equivalent C_1 TSs. Unlike for the C_2 saddle points, the nature of the minima connected by the C_1 TS is not immediately obvious. We verified the nature of this TS by constructing the intrinsic reaction coordinate (IRC). The IRC passing through the C_1 TS connects the bridged C_{2v} $B_2I_4(\mu\text{-}I)_2$ minimum to (an approximately C_2-symmetric) van der Waals dimer. Compared to the C_2 saddle point, the C_1 B_2I_6 TS is lowered by about 8.8 kJ/mol at the MP2 level. Inclusion of a single-point CCSD(T) correlation correction reverses the relative stability of the C_1 and C_2 TSs, with the C_2 saddle-point becoming more stable by about 9.4 kJ/mol (Table 2). Reoptimization of the C_2 TS at the CCSD(T)/cc-pVTZ level leaves the dissociation barrier essentially unchanged (Table 2).

Overall, the $B_2I_4(\mu\text{-}I)_2$ dissociation TS should be close to the C_2 symmetry and is expected to be very anharmonic with respect to the antisymmetric combination of the stretching vibrational modes of the separating B−I bonds. The height of the barrier (14 kJ/mol being our best estimate of the barrier height) may be sufficient to allow isolation of the bridged $B_2I_4(\mu\text{-}I)_2$ dimers in the cryogenic matrix or in a suitable carcerand host.

Table 1. Selected Structural Parameters and Heats of Formation (kJ/mol) for Covalent-Bridged $B_2X_4(\mu\text{-}X)_2$ Dimer Species[a]

X	sym[b]	N_{imag}[c]	CCSD(T)[d]	MP2[e]	$R_{B-X(b)}$	$R_{B-X(t)}$	$\varphi_{B-X-X-B}$
F	D_{2h}	0	39.8	40.2	1.538	1.314	180.0
Cl	C_{2v}	0	59.7	45.5	1.962	1.762	163.2
	D_{2h}	1	59.6	45.7	1.961	1.763	180.0
Br	C_{2v}	0	34.6	13.6	2.104	1.917; 1.919	155.6
	D_{2h}	1	35.3	15.0	2.101	1.919	180.0
I	C_{2v}	0	14.9[f]	−13.6	2.309[f]	2.154; 2.156[f]	149.4[f]
	D_{2h}	1	17.9	−9.2	2.306	2.157	180.0

[a] For B−X distances, b denotes bridging and t denotes terminal. Distances are in angstroms; dihedral angles are in degrees. [b] Point-group symmetry of the structure. [c] Number of imaginary frequencies in MP2/cc-pVTZ harmonic vibrational analysis. [d] MP2/cc-pVTZ energy (including ZPE correction), with CCSD(T)/cc-pVDZ correlation correction; see the text. [e] MP2/cc-pVTZ energy, including harmonic ZPE vibrational correction. [f] Reoptimization at the CCSD(T)/cc-pVTZ level yields a structure with $R_{B-X(bridge)} = 2.329$ Å, $R_{B-X(terminal)} = 2.168$ and 2.169 Å, and $\varphi_{B-X-X-B} = 152.2°$. The CCSD(T)/cc-pVTZ heat of formation, including CCSD/cc-pVDZ ZPE, is 21.8 kJ/mol.

Table 2. TSs for Dissociation of $B_2X_4(\mu\text{-}X)_2$ Dimers in the Gas Phase

X	sym	N_{imag}	CCSD(T)[a]	MP2[b]	R_{B-X}[c]
Cl	C_2	1	2.5	5.0	2.215
Br	C_2	1	6.3	11.3	2.435
I	C_2	2	14.1[d]	23.8[c,d]	2.755[c,d]
	C_1	1	23.5	15.0	2.961; 2.487

[a] MP2/cc-pVTZ energy (including ZPE), with CCSD(T)/cc-pVDZ correlation correction, see the text. [b] MP2/cc-pVTZ energy, including ZPE. Imaginary normal modes are excluded from ZPE evaluation; see the text. [c] Length of the dissociating B−X bonds in angstroms. [d] Re-optimization at the CCSD(T)/cc-pVTZ level yields $R_{B-X} = 2.716$ Å and 14.3 kJ/mol activation barrier (including CCSD/cc-pVDZ ZPE). The projected CCSD/cc-pVDZ Hessian at the CCSD(T)/cc-pVTZ TS geometry shows two imaginary modes (234*i* and 12*i* cm^{-1}).

dx.doi.org/10.1021/ic2016512 |*Inorg. Chem.* 2011, 50, 10472–10475

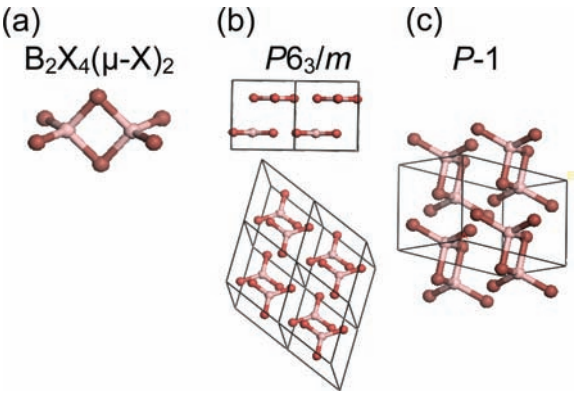

Figure 1. Structure of the (a) D_{2h} gas-phase dimer of BX_3. (b) Ambient-pressure $P6_3/m$ BX_3. (c) Predicted high-pressure $P\bar{1}$ B_2X_6.

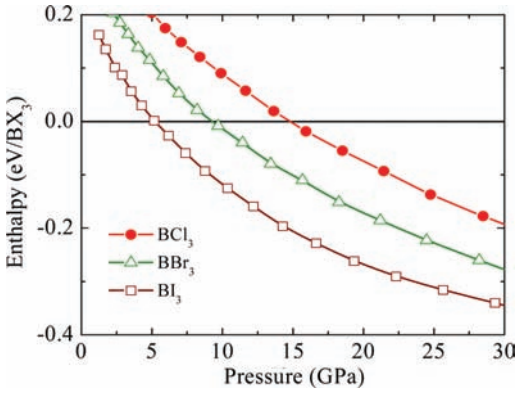

Figure 2. Calculated pressure dependence of the enthalpies of the $P\bar{1}$ structures of B_2Cl_6, B_2Br_6, and B_2I_6 relative to the $P6_3/m$ monomeric solids.

The dimeric $B_2X_4(\mu\text{-}X)_2$ structures correspond to a shallow, but stable local PES minimum for X = Cl, Br, and I (but not F). Formation of the dimers is associated with a significant volume decrease. Can these molecules be stabilized in bulk by applying external pressure?

The structure of the BI_3 dimer and the low- and high-pressure BI_3 crystalline solids are illustrated in Figure 1. Calculated enthalpies for the $P\bar{1}$ structures of each of the BX_3 solids relative to that of the $P6_3/m$ phase are shown in Figure 2 over the pressure range from 0 to 30 GPa. The transition pressure of about 5.4 GPa for the BI_3 $P6_3/m$ phase to the $P\bar{1}$ structure is in good agreement with the recently reported experimental value of 6.2 GPa.[12] Predicted transition pressures for BBr_3 and BCl_3 solids are at 9 and 15 GPa, respectively. It is interesting to note that, for phase transitions in the alkali halides and hydrides, the transition pressures for NaCl- to CsCl-type structures also decreases with increasing alkali-metal atomic number.[24]

The parent $P6_3/m$ phases of the boron trihalides (Figure 1) are layered molecular structures, with the BX_3 moieties located at large intermolecular separations. The new $P\bar{1}$ structures are obtained by compaction of the neighboring planes in the hexagonal structure. The BX_3 fragments simultaneously undergo small, local translation within the plane, positioning one of the X atoms immediately above the boron in the nearest-neighboring plane.[13] This transformation yields a distorted face-centered lattice for the halogen atoms, with the B atoms populating selected tetrahedral sites, thus forming the dimers (Figure 1). The dihedral angles (B−X−X−B) for dimers in the $P\bar{1}$ solid-state structure are 180°. Although the two heavier dimers (X = Br, I) are predicted to form a distorted C_{2v} structure in the gas phase, the energy differences with the D_{2h} saddle points are small (Table 1), so that the final solid-state structure is strongly affected by packing effects.

Although the $P\bar{1}$ solid of the molecular dimers is thermodynamically preferred at high pressure to the $P6_3/m$ monomer-based solid, is it kinetically accessible? The answer is already evident from the local nature of the structural transformation connecting the two solids. For the BI_3−$B_2I_4(\mu\text{-}I)_2$ system, metadynamics simulations and solid-state reaction path profiles[13] confirm that the dimer solid is accessible and is the kinetically preferred product. For the chloride and bromide species, metadynamics simulations starting with the $P6_3/m$ structures yield $P\bar{1}$ solids at 34 and 50 GPa, respectively.

These transformation pressures are likely overestimated as a result of the computational limitations; larger unit cells and longer simulation times are expected to bring the transformation pressures down, closer to the thermodynamic stability threshold [9 GPa for $B_2Br_4(\mu\text{-}Br)_2$; 15 GPa for $B_2Cl_4(\mu\text{-}Cl)_2$].

Finally, it should be emphasized that the $P\bar{1}$ structure arises from just one of many possible packing arrangements of $B_2X_4(\mu\text{-}X)_2$ dimers. A more careful investigation[13] shows that several alternative dimer arrangements with nearly identical total energies are possible as well. Although the $P\bar{1}$ packing discussed presently has the advantage of being formed by the smallest displacement from the $P6_3/m$ monomeric solid, other dimer-based structures may arise under suitable conditions.

The present study provides a theoretical characterization of the structures and stabilities of dimers of BX_3 in the gas and solid phases. The results indicate that the gas-phase dimer structures are possibly stable only near 0 K or perhaps containable in an inclusion compound. Nonetheless, these molecules can be prepared straightforwardly in the solid at high, but experimentally accessible, pressure. The high-pressure solid structures of BBr_3 and BCl_3 are predicted to be described by the $P\bar{1}$ space group, as has recently been found for BI_3.[13] The high-pressure $P\bar{1}$ $B_2X_4(\mu\text{-}X)_2$ molecular solids are the kinetically preferred product of compression of the ambient-pressure molecular BX_3 solids. Dimerization in the high-pressure phases of BBr_3 and BCl_3 is suggested to result from a transformation that involves a uniaxial compression of the hexagonal $P6_3/m$ structure combined with translation of BBr_3 or BCl_3 molecular components, as was found for BI_3[13] to yield structures where a basic dimer motif is obtained.

The new binary boron(III) halides, which, if experimentally confirmed, will be the first new isolable species in their class since the end of the 19th century,[14] open new possibilities for studying boron in unusual bonding environments. These species permit a direct experimental investigation of the delicate balance between π back-donation and σ donation in electron-deficient molecules. Furthermore, the very simple synthetic approach we propose for preparing these species highlights the so far largely overlooked control parameter of the chemical reactivity of condensed systems: the externally applied pressure.

AUTHOR INFORMATION

Corresponding Author

*E-mail: Yansun.Yao@nrc.ca.

REFERENCES

(1) Morrison, J. A. *Chem. Rev.* **1991**, *91*, 35–48.

(2) Bunce, S. J.; Edwards, H. G. M.; Lewis, I. R.; Smith, D. N. *J. Mol. Struct.* **1994**, *320*, 57–64.

(3) Edwards, H. G. M.; Fawcett, V.; Price, G. P. J. *J. Mol. Struct.* **1990**, *220*, 227–234.

(4) Nxumalo, L. M.; Ford, T. A. *Vib. Spectrosc.* **1994**, *6*, 333–343.

(5) Nxumalo, L. M.; Ford, T. A. *J. Mol. Struct.* **1993**, *300*, 325–338.

(6) Williams, S. D.; Harper, W.; Mamantov, G.; Tortorelli, L. J.; Shankle, G. *J. Comput. Chem.* **1996**, *17*, 1696–1711.

(7) Cotton, F. A.; Wilkinson, G.; Murillo, C. A. Bochmann, M. *Advanced Inorganic Chemistry*, 6th ed.; Wiley-Interscience: New York, 1999.

(8) Ownby, P. D.; Gretz, R. D. *Surf. Sci.* **1968**, *9*, 37–56.

(9) Santiso-Quiñones, G.; Krossing, I. *Z. Anorg. Allg. Chem.* **2008**, *634*, 704–707.

(10) Atoli, M.; Lipscomb, W. N. *J. Chem. Phys.* **1957**, *27*, 195. Ring, M. A.; Donnay, J. D. H.; Koski, W. S. *Inorg. Chem.* **1962**, *1*, 109. Spenser, C.; Lipscomb, W. N. *J. Chem. Phys.* **1958**, *28*, 355.Wyckoff, R. W. G. *Crystal Structures*; Wiley-Interscience: New York, 1964; Vol. 2.

(11) Anderson, A.; Lettress, L. *J. Raman Spectrosc.* **2002**, *33*, 173–176. Anderson, A.; Lettress, L. M. *J. Raman Spectrosc.* **2003**, *34*, 684–687.

(12) Hamaya, N.; Ishizuka, M.; Onoda, S.; Guishan, J.; Ohmura, A.; Shimizu, K. *Phys. Rev. B* **2010**, *82*, 094506.

(13) Yao, Y.; Klug, D. D.; Martonak, R.; Patchkovskii, S. *Phys. Rev. B* **2011**, *83*, 214105.

(14) Moissan, H. *Comptes Rendus* **1891**, *112*, 717–720.Morrison, J. A. In *Advances in boron and boranes*; Burg, A. B., Liebman, J. F., Greenberg, A., Williams, R. E., Eds.; VCH: New York, 1988; pp 151−189.

(15) Amrutha, R.; Sangeetha, L.; Samuel, D.; Chandran, P. *Indian J. Chem.* **2002**, *41A*, 1329–1333.

(16) Dunning, T. H., Jr. *J. Chem. Phys.* **1989**, *90*, 1007–1023. Woon, D. E.; Dunning, T. H., Jr. *J. Chem. Phys.* **1993**, *98*, 1358–1371.

(17) Peterson, K. A.; Figgen, D.; Goll, E.; Stoll, H.; Dolg, M. *J. Chem. Phys.* **2003**, *119*, 11113–11123. Peterson, K. A.; Shepler, B. C.; Figgen, D.; Stoll, H. *J. Phys. Chem. A* **2006**, *110*, 13877–13883.

(18) Stanton, J. F.; Gauss, J.; Harding, M. E.; Szalay, P. G. CFOUR, Coupled-Cluster techniques for Computational Chemistry, 2011, http://www.cfour.de.

(19) Bentz, J. L.; Olson, R. M.; Gordon, M. S.; Schmidt, M. W.; Kendall, R. A. *Comput. Phys. Commun.* **2007**, *176*, 589–600.Gordon, M. S.; Schmidt, M. W. In *Theory and Applications of Computational Chemistry, the First Forty Years*; Dykstra, C. E., Frenking, G., Kim, K. S., Scuseria, G. E., Eds.; Elsevier: Amsterdam, The Netherlands, 2005; pp 1167−1189; Piecuch, P.; Kucharski, S. A.; Kowalski, K.; Musial, M. *Comput. Phys. Commun.* **2002**, *149*, 71–96. Schmidt, M. W.; Baldridge, K. K.; Boatz, J. A.; Elbert, S. T.; Gordon, M. S.; Jensen, J. H.; Koseki, S.; Matsunaga, N.; Nguyen, K. A.; Su, S.; Windus, T. L.; Dupuis, M.; Montgomery, J. A. *J. Comput. Chem.* **1993**, *14*, 1347–1363.

(20) Kresse, G.; Hafner, J. *Phys. Rev. B* **1993**, *47*, 558–559. Kresse, G.; Joubert, D. *Phys. Rev. B* **1999**, *59*, 1758–1775.

(21) Perdew, J. P.; Burke, K.; Ernzerhof, M. *Phys. Rev. Lett.* **1996**, *77*, 3865–3868.

(22) Gonze, X.; Beuken, J. M.; Caracas, R.; Detraux, F.; Fuchs, M.; Rignanese, G. M.; Sindic, L.; Verstraete, M.; Zerah, G.; Jollet, F.; Torrent, M.; Roy, A.; Mikami, M.; Ghosez, P.; Raty, J. Y.; Allan, D. C. *Comput. Mater. Sci.* **2002**, *25*, 478–492.

(23) Krack, M. *Theor. Chem. Acc.* **2005**, *114*, 145–152. Troullier, N.; Martins, J. *Phys. Rev. B* **1991**, *43*, 1993–2006.

(24) Hochheimer, H. D.; Strössner, K.; Hönle, W.; Baranowski, B.; Filipek, F. *Z. Phys. Chem. (München)* **1985**, *143*, 139–144.